BIOCHEMISTRY
including biophysical chemistry & molecular biology

Article

pubs.acs.org/biochemistry

The D1-D61N Mutation in *Synechocystis* sp. PCC 6803 Allows the Observation of pH-Sensitive Intermediates in the Formation and Release of O_2 from Photosystem II

Preston L. Dilbeck,[†] Hong Jin Hwang,[†] Ivelina Zaharieva,[‡] Laszlo Gerencser,[‡] Holger Dau,[‡] and Robert L. Burnap*[,†]

[†]Department of Microbiology and Molecular Genetics, Oklahoma State University, Stillwater, Oklahoma 74078-4034, United States
[‡]Department of Physics, Free University Berlin, Berlin, Germany

Supporting Information

ABSTRACT: The active site of photosynthetic water oxidation by Photosystem II (PSII) is a manganese−calcium cluster (Mn_4CaO_5). A postulated catalytic base is assumed to be crucial. CP43-Arg357, which is a candidate for the identity of this base, is a second-sphere ligand of the Mn_4−Ca cluster and is located near a putative proton exit pathway, which begins with residue D1-D61. Transient absorption spectroscopy and time-resolved O_2 polarography reveal that in the D1-D61N mutant, the transfer of an electron from the Mn_4CaO_5 cluster to Y_Z^{OX} and O_2 release during the final step of the catalytic cycle, the S_3−S_0 transition, proceed simultaneously but are more dramatically decelerated than previously thought ($t_{1/2}$ of up to ∼50 ms vs a $t_{1/2}$ of 1.5 ms in the wild type). Using a bare platinum electrode to record the flash-dependent yields of O_2 from mutant and wild-type PSII has allowed the observation of the kinetics of release of O_2 from extracted thylakoid membranes at various pH values and in the presence of deuterated water. In the mutant, it was possible to resolve a clear lag phase prior to the appearance of O_2, indicating formation of an intermediate before the onset of O_2 formation. The lag phase and the photochemical miss factor were more sensitive to isotope substitution in the mutant, indicating that proton efflux in the mutant proceeds via an alternative pathway. The results are discussed in comparison with earlier results obtained from the substitution of CP43-Arg357 with lysine and in regard to hypotheses concerning the nature of the final steps in photosynthetic water oxidation. These considerations led to the conclusion that proton expulsion during the initial phase of the S_3−S_0 transition starts with the deprotonation of the primary catalytic base, probably CP43-Arg357, followed by efficient proton egress involving the carboxyl group of D1-D61 in a process that constitutes the lag phase immediately prior to O_2 formation chemistry.

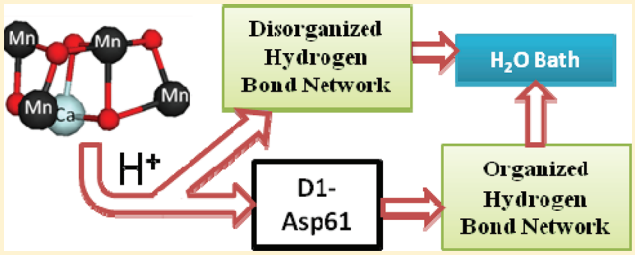

The H_2O oxidation complex (WOC) of Photosystem II (PSII) catalyzes the oxidation of water by coordinating the extraction of both protons and electrons from the substrate H_2O molecules. The process is mechanistically complicated because the oxidation of two water molecules and the formation of molecular oxygen require the extraction of four protons and four electrons from a pair of substrate H_2O molecules. Moreover, the univalent photochemistry of the PSII reaction center can extract only one electron per photocycle. A model describing the accumulation of oxidizing equivalents by the WOC was developed by Kok et al.[1] on the basis of the observation that under a series of brief (<10 μs) saturating flashes a dark-adapted sample of PSII releases O_2 in an oscillating pattern with a periodicity of 4.[2] In this model, known as the "S-state cycle", each charge separation at the photochemical reaction center causes the WOC to advance through a repeating series of oxidation states, called S states, designated S_0−S_4 according to the number of stored oxidizing equivalents (for reviews, see refs 3−7). The final S_4 state is a transient state formed by the fourth oxidation step that precedes the formation of O_2 and the return of the WOC to the S_0 state. The transient S_4 state [or S_3^n (see ref 7] appears to form within <200 μs of the flash[8−11] and is followed by the formation of dioxygen in approximately 1000 μs (half-time), making the overall S_3−S_0 transition the slowest of the S-state transitions. Dark-adapted samples of PSII display maximal O_2 yields after the third flash in a series of flashes because of the dark stability of the S_1 state. The accumulation of oxidizing equivalents is facilitated by a cluster of four Mn ions and one Ca ion with five μ-oxo bridges (Mn_4CaO_5), which act as an interface between the photochemical reactions and the substrate water.[12] The well-coordinated removal of both protons and electrons from the metal complex and its ligand environment is, among other things, mechanistically crucial, facilitating successive one-electron oxidation of the Mn complex without a prohibitive

Received: November 2, 2011
Revised: December 21, 2011
Published: December 22, 2011

increase in its oxidation potential by appropriate redox potential leveling.[5,11,13]

Crystal structures of PSII reveal a putative hydrophilic channel that could plausibly serve as a proton exit pathway from the WOC to the lumen of the thylakoid membrane.[14,15] This pathway includes the titratable residues D1-Asp61, D1-Glu65, D2-Lys317, D2-Glu312, PsbO-Asp158, PsbO-Asp222, PsbO-Asp223, PsbO-Asp224, PsbO-His228, and PsbO-Glu229. Computational analysis[16] based on the crystal structure of PSII indicates that the pK_a of each of these residues, along with D1-Asp59, D1-Arg64, and PsbO-Arg152, increased with the distance from Mn_4CaO_5 and toward the lumenal surface of the protein. The calculations further suggest that the pK_a's are dramatically influenced by deprotonation of CP43-Arg357, the putative catalytic base necessary for the initial removal of protons from substrate H_2O.[8,17,18] Several of these residues (D1-Asp61, D1-Glu65, D1-Asp59, D2-Lys317, and D2-Glu312) also come into contact with the putative water channels that connect the Mn_4CaO_5 with the proteins surface, which presents the possibility that ordered H_2O molecules also play a role in the proposed proton exit pathways.[14,19−21] Tests of this hypothesis regarding the proton efflux pathway(s) have yet to be made.

The residue closest to Mn_4CaO_5 in any of the proposed proton exit pathways is D1-Asp61 (D1-D61), an aspartate residue in the second coordination sphere of the Mn_4CaO_5 cluster[14,15] shown in Figure 1. D1-D61 is positioned ~6 Å from

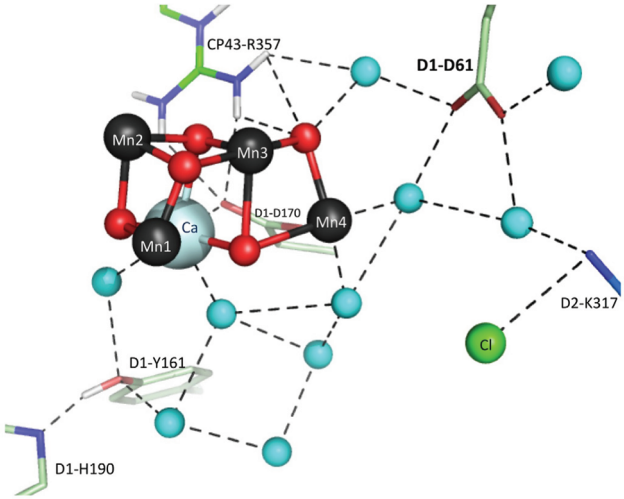

Figure 1. Mn_4CaO_5 cluster of photosystem II showing several key amino acid residues and water molecules (cyan spheres) in the environment of the metal cluster.[12] Second-sphere side chain ligands, D1-Asp61 and CP43-Arg357, are proposed to mediate the transfer of protons from the active site.

CP43-Arg357, which has been proposed to serve as a catalytic base in PSII water oxidation.[8,17,18] Furthermore, D1-D61 is a second-sphere ligand of Mn_4CaO_5 because it coordinates two waters molecules, one of which is a ligand of the Mn4 atom and the other of which is within hydrogen bonding distance of an oxo bridge of Mn_4CaO_5.[12] D1-D61 and CP43-Arg357 are separated by the so-called narrow channel, one of the putative water channels that connect the Mn_4CaO_5 cluster with the lumenal surface of PSII.[19,20] The role of D1-D61 has been examined through mutational studies, starting with that of Chu et al., in which mutant strains of the cyanobacterium *Synechocystis* sp. PCC 6803 were created in which D1-D61 was replaced with asparagine, alanine, and glutamate.[22] Subsequently, the D1-D61N mutant was determined to be defective in S-state cycling, most notably having a highly retarded O_2 release kinetic coinciding with a similarly retarded transfer of an electron from the Mn_4CaO_5 cluster to Y_Z^{OX}.[23−25]

The chemical basis for the observed deceleration of the H_2O oxidation reaction in the D1-D61N mutant remains to be established. Because it is proposed to be part of the proton exit pathway and because of its proximity to the Mn_4CaO_5 cluster, it is an interesting target for analysis of potential alterations in proton handling characteristics during H_2O oxidation catalysis. Here we have analyzed the O_2 producing activity of mutant and wild-type membranes at a range of pH and pD values using a bare platinum electrode capable of high time resolution. Our results show that oxygen evolution in the D1-D61N mutant has an altered pattern of pH sensitivity in comparison to that of the wild type and also has a larger isotope effect upon substitution with D_2O. The relation of the slowed O_2 release to the re-reduction of Y_Z^{OX} was confirmed via UV spectroscopy. These results support a model of PSII activity in which trapping of a state immediately prior to Y_Z^{OX} re-reduction and dioxygen formation depends upon ejection of a proton mediated by D1-D61. However, the results also indicate that the role of D1-D61 in facilitating dioxygen formation extends beyond proton transfer alone.

EXPERIMENTAL PROCEDURES

Strains and Growth Conditions. The naturally transformable, glucose-tolerant strain of *Synechocystis* sp. PCC6803 was maintained on solid BG-11 and in liquid BG-11 buffered with 20 mM Hepes-NaOH (pH 8.0) supplemented with 5 mM glucose and 10 μM DCMU (solid media only). Experimental cultures were illuminated with ~70 μmol m^{-2} s^{-1} Cool White fluorescent lights with bubbling filter sterilized air, enriched with ~3% CO_2. A LiCor (Lincoln, NE) photometer was used to measure the light intensity. The D1-D61N mutation was constructed in the *psbA2* gene and introduced into a recipient strain of *Synechocystis* lacking all three *psbA* genes and containing a hexahistidine "tag" genetically fused to the C-terminus of the CP47 protein.[22,26] A hexahistidine-tagged control strain was similarly constructed using the same *psbA*-less, recipient strain but transformed with the wild-type *psbA2* gene, resulting in a strain possessing PSII activity similar to that of the true wild type,[26] and is called the wild type.

Isolation of Thylakoid Membranes. Thylakoid membranes were isolated essentially as described previously.[27−29] *Synechocystis* cells were harvested by centrifugation for 10 min at 8000*g* and then resuspended in 50 mM MES-NaOH (pH 6.0), 10% (v/v) glycerol, 1.2 M betaine, 5 mM $MgCl_2$, and 5 mM $CaCl_2$ to a chlorophyll concentration of 1 mg/mL. The resuspended cells were incubated in the dark and on ice for 1 h. Prior to cell breakage, benzamidine, ε-amino-η-caproic acid, and phenylmethanesulfonyl fluoride were added to the cell suspension to a concentration of 1 mM each. The cells were broken by five cycles (5 s on and 5 min off) of agitation with 0.1 mm diameter zirconium/silica beads in a Bead-Beater (BioSpec Products, Bartlesville, OK) in a water-ice jacket. Unbroken cells and suspended zirconium/silica beads were removed by centrifugation at 3500*g* for 10 min at 4 °C. The extracted thylakoid membranes were collected by centrifugation at 40000 rpm for 20 min at 4 °C in a Beckman 70Ti rotor. The pelleted thylakoid membranes were resuspended in 50 mM

dx.doi.org/10.1021/bi201659f | *Biochemistry* 2012, 51, 1079−1091

MES-NaOH (pH 6.0), 10% glycerol (v/v), 1.2 M betaine, 20 mM $CaCl_2$, and 5 mM $MgCl_2$ to a Chl concentration of 1−1.5 mg/mL, before being flash-frozen in liquid nitrogen and stored at −80 °C.

Isolation of PSII Core Particles. Histidine-tagged PSII core particles were extracted from thylakoid membranes using previously described procedures.[27−29] Thylakoid membranes were solubilized by adding 1% (w/v) *n*-dodecyl *β*-D-maltoside to the resuspension buffer while the sample was being stirred on ice. Insoluble material was removed from the membrane extract by centrifugation at 22300 rpm for 10 min at 4 °C in a Beckman 70Ti rotor. The resulting supernatant was pumped onto a 2.6 cm diameter column of Ni-NTA Superflow (Qiagen, Inc.) affinity resin with a peristaltic pump at a rate of 1.5 mL/min in a darkened cabinet at 4 °C to facilitate binding of the His-tagged PSII complexes to the affinity resin. The column was washed with 50 mM MES (pH 6.0), 10% (v/v) glycerol, 1.2 M betaine, 5 mM $MgCl_2$, 20 mM $CaCl_2$, and 0.03% *n*-dodecyl *β*-D-maltoside. The PSII complexes bound to the affinity column were eluted with buffer containing 50 mM L-histidine, 50 mM MES (pH 6.0), 10% (v/v) glycerol, 1.2 M betaine, 5 mM $MgCl_2$, 20 mM $CaCl_2$, and 0.03% *n*-dodecyl *β*-D-maltoside. The eluted solution was concentrated in two stirred ultrafiltration cells (first in a 400 mL cell and then in a 10 mL cell) (Amicon YM-100 membranes under 60 psi N_2 at 4 °C) to a final Chl concentration of 1−1.5 mg/mL.

Polarographic Measurements of O_2 Evolution. Measurement of flash number-dependent O_2 yields and O_2 release kinetics was performed with isolated thylakoid membranes using a bare platinum electrode that allows for the deposition of samples by centrifugation as described previously.[30−33] For each measurement, a sample of thylakoid membranes containing 3 *μ*g of chlorophyll was added to 500 *μ*L of 50 mM MES-NaOH (pH 4.0−8.0), 1 M sucrose, 200 mM NaCl, and 10 mM $CaCl_2$. The pD was calculated as pD_{read} + 0.4, where pD_{read} is the pH meter reading. Samples were centrifuged onto the electrode surface at 10500*g* for 10 min at 20 °C in a Sorvall HB-4 swing out rotor. The temperature of the electrode was regulated by circulating thermostated water through a copper jacket that surrounds the electrode. Polarization of the electrode (0.73 V) was initiated 20 s before the start of data acquisition, and the flash sequence was initiated 333 ms after that. The response time of the polarographic amplifier is approximately 100 *μ*s, whereas the electrode−electrolyte system responds within approximately 200−400 *μ*s at the specified NaCl concentration in the measuring buffer. Acquisition of the data and the control of the instrumentation were implemented using a plug-in data acquisition circuitry and software (National Instruments) that permitted timing and coordination of the flash illumination and data acquisition in a synchronous mode with nanosecond accuracy (independent of computer motherboard and operating system). The timing of the flash points relative to the O_2 signals and instrument response time was verified in separate trials by observing the photoelectric signal resulting from exposing the silver electrode to unfiltered xenon flashes. Samples were allowed to thermally equilibrate to the temperature of the water jacket for 10 min on the electrode receiver before data acquisition was initiated. This proved to be critical in obtaining reproducible oxygen signal decay transients because of their strong temperature dependence, especially in the rate of the decay of the O_2 signal.

Measurements of O_2 release patterns for the determination of the S-state cycling parameters (hit, miss, double-hit frequencies) utilized a xenon flash lamp that provides saturating flashes with a duration of approximately 6 *μ*s at full intensity signal width, half-maximal amplitude. Prior to centrifugation, the thylakoid membrane samples were exposed to normal room light for 30 s to provide samples uniformly populated among the S states and to promote homogeneity with respect to the redox state of secondary donors such as Y_D. The samples were centrifuged for 10 min in the dark. After centrifugation, the samples were exposed to a single saturating flash from a xenon lamp and then dark-adapted for 10 min to increase the fraction of PSII centers in the S_1 state. Samples were given a series of 19 flashes at a frequency of 1 Hz, and the resulting oscillatory pattern of O_2 release was analyzed using a four-state model.[31,34]

For measurements of the flash-induced O_2 release kinetics (rate of appearance of O_2 at the electrode), a different procedure was used. The electronic disturbance from the discharge of the xenon flash lamp proved to be problematic for measurements of early time points after the flash artifact. This is due to a polarographic current artifact that the discharge induced together with the photoelectric effect as described previously.[23] Therefore, an alternative form of flash illumination using a high-intensity light-emitting diode (LED) was employed, which minimized this flash artifact. Samples were exposed to a train of 50 *μ*s flashes from a red (nominally 627 nm) Luxeon III Emitter LED (Philips Electronics) driven by a strobe current generator (Pulsar 710, Advanced Illumination, Rochester, VT), placed 0.9 cm from the surface of the electrode given at 2 Hz after allowing the sample and electrode to temperature equilibrate to 30 °C. Each sample was exposed to up to 600 flashes, and the signals were averaged. The kinetics of the O_2 release curves were fit to a custom-made numerical model that takes into account the production of O_2, the diffusion of O_2 between different layers of the thylakoid membrane sample and toward the aqueous bulk, and the consumption of O_2 by the surface of the bare platinum electrode in the lowest membrane layer (see the Supporting Information for a description of the mathematical model). Varied interval double-flash procedures were used to calculate the rate of PSII turnover.[32,35] For these measurements, samples were exposed to LED flashes at 2 Hz with the exception of the fourth flash, which was given after a variable time period.

Measurement of Absorption Changes at 360 nm. The transfer of an electron from the Mn_4CaO_5 cluster to Y_Z^{OX} was monitored by time-resolved absorption measurements at 360 nm. Core particles were diluted to 10 *μ*M (chlorophyll concentration) in a buffer with 10% glycerol, 0.03 dodecyl *β*-D-maltoside, 1 M betaine, 25 mM MES (pH 6.2), 10 mM NaCl, 5 mM $CaCl_2$, and 5 mM $MgCl_2$; 100 *μ*M DCBQ and 500 *μ*M potassium ferricyanide were added as artificial electron acceptors. The absorption transients induced by flash series (flash spacing of 375 ms) were collected with a 100 kHz electrical bandwidth, and 20 traces were averaged to increase the signal-to-noise ratio. The monochromatic measuring light was transmitted through the sample to the surface of the photocathode of the photomultiplier (electron tubes, 9734B). The slow excitation of the sample by measuring light was circumvented by a photoshutter operating in front of the sample. The photomultiplier was protected from the scattered laser and prompt fluorescent light by a combination of interference (Asahi spectra, ASA ZBPA 360) and band-pass (Schott, BG3) filters. The sample was excited perpendicular to the measuring beam by frequency-doubled, Q-switched Nd-Systems, SR560, and the signal was digitized (Adlink PCI-

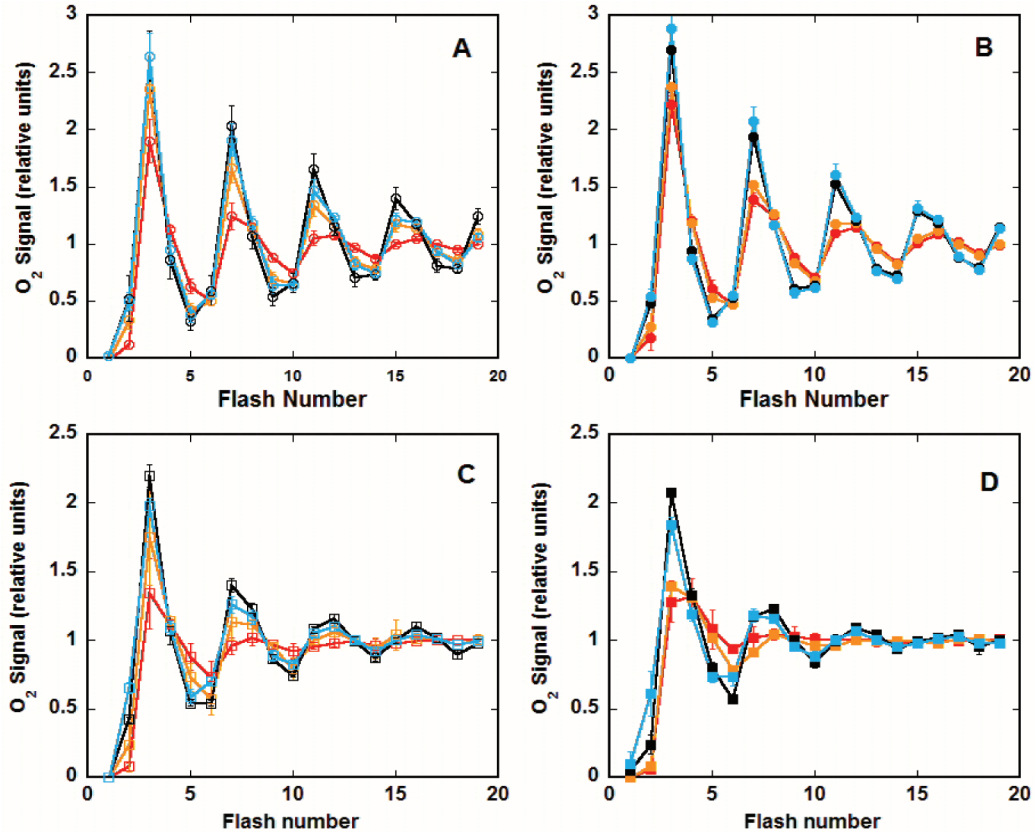

Figure 2. Flash-dependent O_2 yields as a function of flash number. Samples of thylakoid membranes were given a single saturating flash and dark-adapted for 10 min before being exposed to 19 saturating flashes from a xenon lamp at 1 Hz while being kept at a constant temperature of 20 °C. Panel A shows the yield of O_2 from the wild type at pH 5.0 (red), 5.5 (orange), 6.5 (black), and 7.5 (blue). Panels B–D show the O_2 yields from the wild type in D_2O buffer, D1-D61N in H_2O buffer, and D1-D61N in D_2O buffer, respectively. Each point represents the average of at least three measurements. The amplitudes from each measurement were normalized to the average amplitude of the last four flashes. Error bars represent the standard deviation of the normalized O_2 yields from three samples.

9812). Actinic illumination was provided by a YAG laser (Quantel BrilliantB, 532 nm, 5 ns). The intensity of the laser light was adjusted with a Glan-Taylor prism to the level, which provided saturating excitation of the sample (21 mW/cm^2). The anode voltage signal of the photomultiplier was amplified and filtered by a differential low-noise preamplifier (Stanford Research by home-written software). The analysis of the absorption transients and the modeling of the four-period oscillation were conducted with MathCAD 2001 Professional and Origin 7.5.

RESULTS

pH Dependence of S-State Cycling. The patterns of flash-induced O_2 production in dark-adapted thylakoid membranes were measured as a function of pH and deuterium isotope exchange to assess the proposed role of D1-Asp61 as a mediator of efflux of protons from the H_2O oxidation reaction. A period 4 oscillatory pattern of O_2 release, with a maximum on the third flash, was observed in all samples upon exposure to a series of measuring flashes from a xenon discharge lamp (Figure 2A,C). Samples measured at pH 6.5 exhibited the most sustained oscillations for both the mutant and the wild-type control (Figure 2A,C, black). Assuming a four-S-state model[31,34] and plotting the miss factor as a function of pH show that the miss factor is weakly sensitive to pH in the range of conditions employed (Figure 3, empty symbols). The D1-D61N mutant showed a higher miss factor in comparison to

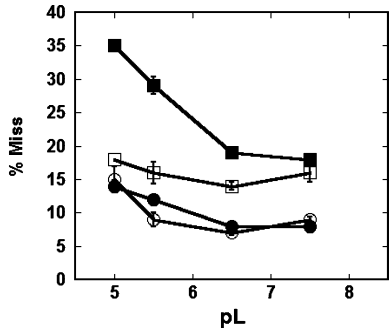

Figure 3. Percent of missed S-state transitions as a function of pH or pD level. Wild-type (circles) and D1-D61N (squares) thylakoid membranes were dark-adapted for 10 min after being exposed to a single saturating flash. The samples were then exposed to 19 measuring flashes. The measurements were repeated with a range of pH (empty circles and empty squares) and pD (filled circles and filled squares) values. Each percent miss was derived by analysis of the amplitudes using a four-state model. Error bars represent the standard deviation of the percentage of failed S-state transitions from three samples for each condition.

that of the wild type at each pH tested. The estimated miss factors for wild-type and D1-D61N thylakoids in pH 6.5 buffer were 7 and 14%, respectively (Figure 3). The general conclusion that the D1-D61N mutation results in an increased miss factor is consistent with in vivo measurements.[24] However,

dx.doi.org/10.1021/bi201659f | *Biochemistry* 2012, 51, 1079–1091

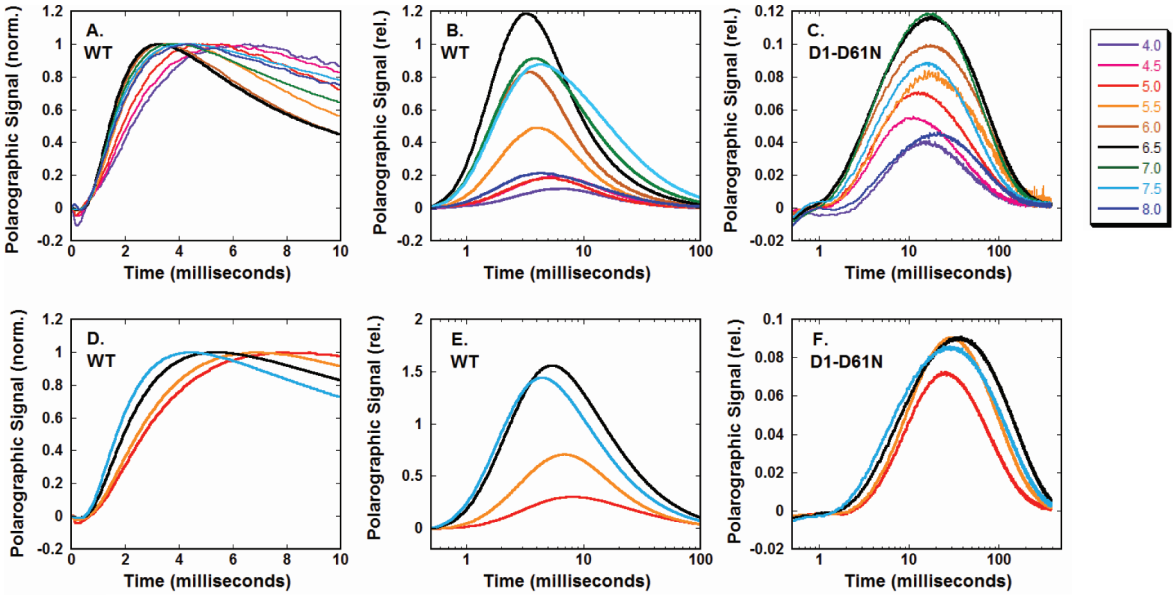

Figure 4. Oxygen release kinetics of wild-type and D1-D161N thylakoid membranes. Membranes were measured at pH 4.0 (purple), 4.5 (pink), 5.0 (red), 5.5 (orange), 6.0 (brown), 6.5 (black), 7.0 (green), 7.5 (light blue), and 8.0 (dark blue) (A–C) and at pD 5.0, 5.5, 6.5, and 7.5 (D–F). The signals shown are the averaged O_2 release signals resulting from 117–600 individual flashes excluding the first three initial flashes in each series of flashes.

the miss factors in those in vivo experiments were considerably higher for both the wild type and the mutant (17 and 26%, respectively),[24] which can be explained by reduced quinone acceptors in living cells.[31,36] A miss factor that is as low as 7% is advantageous as it implies that the acceptor side contribution to the miss factor is negligibly small. The higher miss factors in the mutant are therefore caused by the decreased efficiency of trapping oxidant within the WOC and support the hypothesis that D1-D61 facilitates the release of protons from the WOC as part of the oxidant trapping mechanism.

While the miss factor for S-state advancement in D1-D61N membranes was uniformly higher than that of the wild type under all pH conditions, it did exhibit less sensitivity to differences in pH in the pH range of 5–7.5 than the wild type (in Figure 3, compare empty symbols representing pH buffers). The miss factor in D1-D61N membranes increases only a few percent outside of the pH 6.5 optimum, whereas the wild-type miss factor approximately doubles at pH 5.0 compared to the pH 6.5 optimum. Therefore, the wild-type PSII centers are proportionally more sensitive to changes in the concentration of external protons, although the mutant has a higher miss factor at all tested pH values. This is not unlike the effect of mutating a proton shuttle residue in the carbonic anhydrase active site, which, besides slowing the enzyme, also has the effect of flattening its pH dependence curve.[37,38]

H_2O versus D_2O Isotope Effects on S-State Cycling in D1-D61N and Wild-Type Thylakoid Membranes. To further examine how the D1-D61N mutation affects the O_2 evolving properties of PSII in relation to proton transfer characteristics, the effects of a heavy proton (^2H, alternatively, D) isotope on S-state cycling were determined (Figure 2B,D). The kinetic isotope effect (KIE) on the miss parameter, defined as (miss factor in D_2O)/(miss factor in H_2O), for the wild type was essentially negligible as shown in Figure 3, which shows the miss factor as a function of pL (pH or pD, compare empty and filled circles), consistent with previous observations in spinach.[39] In contrast, deuterated buffer increased the miss factor in the mutant, especially at acidic pL values (in Figure 3, compare empty and filled squares). This indicates that the proton release D1-D61N mutant follows an alternate pathway compared to that of the wild type. The most dramatic decrease in the efficiency of the S-state transition and the largest KIE were observed at low pL values in the mutant. At pL 5.0, the KIE was approximately 2.5 in the mutant, while the KIE decreased at more alkaline pL values, with a negligible isotope effect observed at pL 7.5 (Figure 3, filled vs empty squares). Because the KIE in the mutant is pL-dependent, it is not likely to be a primary isotope effect involving the breaking of a bond transiently retaining the exiting proton on a titratable moiety along a single exit pathway because a significant isotope effect would be expected at all pL values and this is not observed. Instead, the pL-dependent KIE in the mutant is more likely a secondary isotope effect involving a titratable group that controls the proton transfer process in the mutant proton conduction pathway. This titratable group appears to have a pK_a in the range of pH ~5 which would be expected to increase by approximately 0.5 pH unit upon binding the heavier deuteron, which is typical of amino acids in a D_2O solution.[40,41] The protonation of this controlling group blocks S-state advancement in the mutant, but not in the wild type because a similar KIE is not observed. We conclude that the mutation causes defect in the normal proton release mechanism, and proton release instead follows an alternative path.

Determining O_2 Release Kinetics as a Function of pH. Previous analysis has shown that D1-D61 mutations result in a large retardation of the kinetics of O_2 release during the $S_3 \rightarrow S_0$ transition.[23,24] To test whether the deceleration might be due to alterations in the handling of protons by the enzyme, the postflash kinetics of the appearance of O_2 during the $S_3 \rightarrow S_0$ transition was recorded polarographically under a range of pH conditions (Figure 4). As above, thylakoid membranes from the D1-D61N mutant and the wild type were deposited in a thin layer onto the surface of a bare platinum electrode by high-speed (10500*g*) centrifugation. Note this is a considerably

dx.doi.org/10.1021/bi201659f | *Biochemistry* 2012, 51, 1079–1091

higher centrifugal force than that the 1700*g* centrifugation in previous studies with this mutant[23] and, together with the higher salt concentration, likely accounts for the different signal kinetics obtained here. Illumination was provided by 50 μs red LED flashes. This minimized flash artifacts that are more prominent using the xenon source and interfere with the observation of the onset of the O_2 signal. Furthermore, the absence of blue and ultraviolet light in the LED source prevented significant photodamage and allowed each sample to be exposed to a larger number of flashes, allowing better signal averaging.

All O_2 transients feature an initial lag phase (i.e., a delayed onset of the subsequent rise) followed by a sigmoidal rise to a maximum value and a slow decay toward the preflash level. Lag phase duration, the rise, and the signal decay are generally much slower in the D61N mutant than in WT thylakoids, and these features are sensitive to differences in pH (pD) and to H/D exchange (Figure 5). The remaining flash artifact often

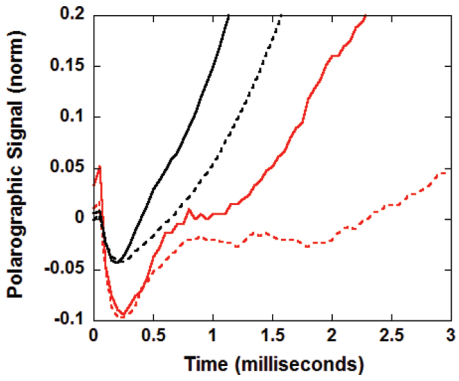

Figure 5. Lag in the onset of O_2 release signals from thylakoid membranes. The onset of release of O_2 from a subset of the averaged O_2 release curves in Figure 4. The D1-D61N thylakoid membranes show a lag in O_2 release in both pH 5.0 buffering solution (solid red line) and a pD 5.0 buffering solution prepared with D_2O (dashed red line). The signals have been normalized to 1.0 at their respective maxima.

resulted in a negative O_2 signal within 400 μs of the LED flash but did not create the observed lag phase behavior. The lag phase duration generally clearly exceeded the previously observed lag phase of ~200 μs detected in UV−vis and X-ray transients.[8−11] The lag phase duration and the extent of sigmoidicity depended strongly on the used polarization voltage (not shown), suggesting a contribution of the O_2 reduction reaction taking place at the bare platinum electrode. Thus, the delayed rise observed in the WT presumably represented the sum of a contribution from the electrode response and a (likely minor) contribution from the reactions in PSII. At present, we cannot disentangle these two contributions. However, lag phase duration and sigmoidicity detected in the WT provide an upper limit for the influence of electrode kinetics on the O_2 transients. In the D1-D61N mutant, the lag phase was longer and the sigmoidicity stronger than those observed in the WT at the same polarization voltage and pH, implying that the delayed rise of the O_2 signal reflects reactions in the D1-D61N mutant that are strongly decelerated in comparison to that of WT PSII (Figure 5).

The wild-type O_2 signal was observed to have the fastest rate of O_2 appearance at pH 6.5 (Figure 4A, black line) in comparison to the signals obtained at other pH levels (Figure 4A, colored lines). Note that the amplitudes of these signals are normalized in panels A and D of Figure 4. The results indicate that, like the maximal rate of O_2 evolution under continuous illumination[27] and the efficiency of S-state advancement as shown above and previously,[42] the release of O_2 during the $S_3 \rightarrow S_0$ transition occurs most rapidly at pH 6.5, consistent with recent results using spinach membranes.[11] The wild-type O_2 signal exhibits a rise half-time of 1.3 ms, as estimated from a basic phenomenological fit of exponential functions to describe the rise and fall of the polarographic signal.[32,43] This value is consistent with previous polarographic estimates of this slowest step of the wild-type S-state cycle[11,32,35,44−46] and is close to the value obtained from data fits using a physical model accounting for O_2 production, diffusion, and consumption at the electrode surface as described below. When samples were suspended in buffers adjusted to pH values on the acidic and basic side of the pH 6.5 optimum, the O_2 signal exhibited a comparative deceleration (Figure 4A, nonblack traces). The most pronounced retardation of the rise of the O_2 signal is observed at pH 4.0 (Figure 4A, purple line), where the apparent half-time is ~2.2 ms, compared to the half-time of the wild-type trace of 1.3 ms. The rise of the signal is distinctly sigmoidal during the initial portion of the rise of the O_2 signal at lower pH values, indicative of a possible kinetic intermediate (pH 4.0 and 4.5, pink and purple curves, respectively, in Figure 4A). This sigmoidicity becomes especially pronounced in the wild type in D_2O (see the next section). Although it is difficult to obtain reproducible amplitudes using a bare platinum electrode, there were observable patterns in the amplitudes of the polarographic signals for membranes suspended at different pH values (Figure 4B). The amplitude of the O_2 signals is routinely observed to be highest at pH 6.5, as seen when representative signals are presented in un-normalized form and on a logarithmic time scale to show the entire signal compactly (Figure 4B, black line). At pH 6.5, the amplitude of the peak of the wild-type O_2 release curve (Figure 4B, black) is ~10-fold higher than the peak of the pH 4.0 curve (Figure 4B, purple). This indicates to a first approximation that the number of PSII centers capable of O_2 evolution is greatly reduced at the extremes of pH because the decrease in the percentage of successful S-state transitions at those pH values is not large enough to account for the great decrease in the per flash O_2 yield. Therefore, we conclude that the wild-type WOC functions optimally at pH ~6.5, with respect to both the speed of the O_2-yielding $S_3 \rightarrow S_0$ transition and (very approximately) the fraction of the population of PSII centers capable of O_2 evolution.

In the case of the D1-D61N mutant, the O_2 release kinetics are greatly slowed compared to those of the wild type as has been observed[23,24] or inferred[22] previously. Here we have expanded upon those observations to test the hypothesis that the delayed release of O_2 from D1-D61N PSII centers is the result of inefficient proton transport (Figure 4C). Surprisingly, values of 4−5 ms for the half-rise times of the O_2 signal were estimated using a basic exponential fit of the signal,[32,43] which is much faster than the previously reported times for this mutant.[23,24] As noted above, the higher centrifugal forces presently used for depositing the membranes on the electrode surface, together with higher salt concentrations here, probably account for the differences. However, estimates of the half-times based on the exponential fit approach greatly underestimate the O_2 release kinetics compared to the case in which the system is physically modeled to account for delays in the decay of the signal due to O_2 diffusion and electrode

consumption, as discussed in the next paragraph. In contrast to the weak dependence of the rise kinetics on pH, the lag period prior to the rise of the O_2 signal in D1-D61N exhibits a strong dependence on pH. Even with the 0.4 ms flash artifact, a clearly visible lag (estimated by inspection of the graph) was observed and ranged from 0.7 to 1.7 ms from the end of the actinic flash to the onset of O_2 release depending on the pH (Figure 4). This lag was shortest (0.7 ms) at pH 6.5 (black) and increased at both higher and lower pH values, reaching 2.0 ms at pH 4.0 (purple) and 1.7 ms at pH 8.0 (dark blue). The existence of a minimum in the duration of the lag centered at pH 6.5 suggests that the titration states of at least two protonatable residues, with pK_a values flanking the optimum, control the rate-limiting process occurring during the lag phase prior to O_2 release in the mutant.

In the D1-D61N mutant and also in other PSII mutants with strongly decelerated O_2 evolution,[32] the retardation of O_2 evolution strongly affects both the rise and the decay of the O_2 signal. The half-time of the O_2 rise depends strongly on the conditions of the electrode experiment, as discussed above, and thus cannot provide a meaningful estimate of the time constant of O_2 formation by PSII. Both the slow signal rise and the drastically increased half-time of the signal decay in D61N (see Figure 4) can be explained by the physical model outlined below.

Quantitative description of the kinetics of O_2 evolution was facilitated by implementation of a physical model[47,48] that takes into account the appearance of O_2 from the enzyme, the diffusive processes governing the concentration of O_2 at the platinum electrode surface, and the electrode reaction consuming O_2 at that surface (Scheme 1). Because the

Scheme 1

$$S_3 \xrightarrow{k_1} I \xrightarrow{k_2} S_0 + O_2$$

occurrence of a lag phase prior to the onset of the rise of the O_2 signal has been observed, most notably in the mutant, the O_2 production terms of the kinetic model include an intermediate, designated "I" for the sake of generality.

At each time point, the model calculates the concentration of O_2 in discrete layers of equal thickness (Δx), which contain either thylakoid membranes or only buffer. The model accounts for the effect of the thickness of the thylakoid membrane sample on the rate of diffusion of O_2 from the electrodes surface by varying the number of thylakoid membrane-containing layers above the bottom layer ($x = 0$). The constant R_{el} refers to the rate of O_2 consumed by the electrode. Equation 1 is used to calculate the concentration of O_2 in the bottom layer ($x = 0$) of the thylakoid membrane sample at each time point t. Aside from the bottom layer ($x > 0$), oxygen diffusion and production (by PSII) are considered but not the oxygen consumption by the electrode. At the top layer, oxygen diffuses into the aqueous bulk. We note that eq 1 describes the delay in the rise of the electrode signal by the rate constant k_1 (k_1 is chosen to be always greater than k_2) and an additional time lag (t_{lag} in eq 1).

$$[O_2]_{x=0}^{t} = [O_2]_{x=0}^{t-\Delta t} + ([O_2]_{x=1}^{t-\Delta t} - [O_2]_{x=0}^{t-\Delta t}) \left(\frac{D}{\Delta x}\right)^2 \Delta t + \frac{k_1 k_2}{k_1 - k_2}[S_3^0][e^{-k_2(t-t_{lag})} - e^{-k_1(t-t_{lag})}]\Delta t - R_{el}[O_2]_{x=0}^{t-\Delta t}\Delta x \quad (1)$$

The time offset (t_{lag}) and k_1 (sigmoidal rise) are used to simulate the overall delay resulting from both the O_2 reduction reaction at the electrode and delayed O_2 production in PSII. The electrode processes are ill-understood and cannot be described sufficiently well by any physicochemical model. This means that the delayed rise of the O_2 signal is described in a purely phenomenological way. Because the values of the two parameters used to describe the delay of the rise of the O_2 signal are strongly correlated, we will report the sum of t_{lag} and k_1^{-1} (see the Supporting Information for further discussion of the O_2 release model).

Application of this model to O_2 transients of WT and D61N resulted in an excellent match of experimental and simulated transients (Figure 6). To verify the diffusion model, the two transients had been simulated using essentially identical parameter values to describe the electrode response (R_{el}) and the thickness of the PSII layer on the Pt electrode. The pronounced differences between the two transients were well reproduced by variation of the half-time for O_2 formation from 1.1 ms (WT) to 31 ms. The astounding difference between the two transients can be understood as follows. In the WT, the production of O_2 is clearly faster than the consumption of O_2 by the electrode. Therefore, O_2 molecules can accumulate in the PSII layer, and the exponential rise of the O_2 concentration results in a concomitant rise in the electrode signal. In the D61N mutant, however, the rate of production of O_2 ($d[O_2]^{produced}/dt$) is small and the formed O_2 is rapidly consumed by the electrode (or diffuses into the aqueous buffer). After an initial equilibration phase (rise of the D61N electrode signal), the exponentially decaying rate of production of O_2 by PSII is reflected in the decay of the electrode signal.

As opposed to the case for the D61N mutant, application of this model to the wild-type signals produced fitting results (Figure 6) that were comparable to the fits produced according to a purely phenomenological fit using exponentials (not shown). The half-times of the faster phase in the wild-type membrane samples became incrementally slower at lower pH values. The slower phase (k_2) was fastest at pH 6.5, which is in harmony with visual inspection of the signals (Figure 4B,C). These trends are more clearly illustrated by plotting the half-times of the phases as a function of pH (Figure 7). The slow phase of O_2 release in wild-type membranes had an optimum at pH 6.5 and became significantly slower at higher and lower pH levels. When the O_2 signals for the D1-D61N mutant were fit according to the physical model, the fast phase (k_1) of release of O_2 from D1-D61N membranes, like that of the wild type, had an optimum at pH 6.5, but they are uniformly slower than the wild type (Figure 7C). The values for the fast phase are consistent with the estimates of the lag obtained by inspection of the graph (Figure 4). The fits using the physical model indicate that the slow phase in D1-D61N membrane samples is at least 1 order of magnitude slower (12−31 ms) than the wild-type slow phase, and qualitatively consistent with previous measurements taken at pH 7.2.[23] However, the slow phase (k_2)

dx.doi.org/10.1021/bi201659f | Biochemistry 2012, 51, 1079−1091

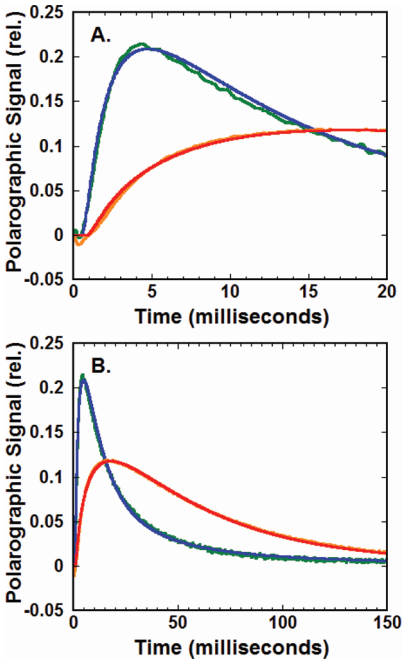

Figure 6. Oxygen release kinetics of wild-type (WT) and D61N thylakoid membranes. Membranes from the wild-type control strain (green) and the D1-D61N mutant (orange) were measured at room temperature (30 °C, pH 6.5, and 200 mM NaCl). In panels A (0−20 ms) and B (0−150 ms), averaged transients (green and orange) and simulations (blue and red) are shown. The simulated lines were obtained by simulation on the basis of a physical model that takes into account oxygen diffusion and consumption of the electrode system used for detection of the oxygen release kinetics. The fits used a custom-made program (by I. Zaharieva), which calculates two rise constants for the release of O_2 as well as the thickness of the TM layer, diffusion processes, and consumption of O_2 at the surface of the electrode. Simulation parameters were optimized by means of a least-squares fit using the electrode reaction parameters for WT and D61N data. The half-times for oxygen evolution are 1.1 and 30.9 ms in WT and D61N, respectively (the complete sets of simulation parameters are shown in Table S1 of the Supporting Information).

of the D1-D61N mutant was paradoxically slowest at more neutral pH values, resulting in an "inverted" optimal curve with respect to the fast kinetic phase.

D_2O Isotope Effects on O_2 Release Kinetics in D1-D61N and Wild-Type Thylakoid Membranes. When wild-type samples are transferred to a D_2O-containing buffer and measured as described above, an overall deceleration of the O_2 signal occurred at all pD values relative to the corresponding pH values (Figures 5 and 7). However, the trends regarding the optimum were slightly different in the presence of deuterons: the fastest release is observed at alkaline values such that pD 7.5 (Figure 7) is the fastest, rather than having an optimum at pH 6.5. Note that the pD 7.5 release was still slower than the pH 6.5 release. These trends are reflected in the slower phase (k_2) of the corresponding fits of the data to the physical model (Figure 7B). D1-D61N thylakoid membranes that were transferred to a D_2O-containing buffer also displayed an overall deceleration of the O_2 signal (Figure 7). The faster phase of the D1-D61N O_2 signals (k_1) has a similar inverse relationship to pD as the slower phase (k_2) of the wild-type O_2 signals, with the optimum at pD 7.5 and becoming slower at lower pD values (Figure 7D).

The KIE of the faster phase of O_2 release (k_1) is highest at pL 5.5 and lowest at pL 7.5 in both the mutant and the wild type. However, unlike the faster phase in the wild type (k_1), which has an almost constant KIE, the KIE of the faster phase in D1-D61N increased sharply at lower pL values (Figure 7C). The pD dependence of the slower phase (k_2) in the mutant O_2 signals has the same inverted pattern as the pH dependence of the signals measured in H_2O, with slower rates near neutral pD values (Figure 7). The pL dependence of the KIE of the D1-D61N slow phase is also inverted in comparison to the pL dependence of the KIE in the wild-type slow phase (Figure 7D). The overall pattern of behavior of the mutant slow phase in relation to proton concentration and isotope appears to be the inverse of the behavior of the mutant fast phase. This may indicate that a new rate-limiting step in the formation of O_2 is introduced by the mutation of Asp61 to asparagine that requires the reversal of a proton transfer that takes place in the earlier phase, or perhaps the filling of a proton hole produced by the removal of a proton from the WOC early in the $S_3 \rightarrow S_0$ transition.

It should be noted that the KIE with a value of 2−3 on the slow phase of O_2 release in the wild type appears to be anomalous compared to published values[11,49,50] of the KIE of the release of O_2 from PSII from spinach, which are in the range of 1.1−1.4. Given that the electrode system presently used is at the margin of kinetic resolution (200−400 μs depending upon the buffer conditions) of the wild-type processes, we tentatively attribute the discrepancy to measuring instrument limitations for the fastest processes of the wild type, although differences in the mechanistic characteristics of spinach versus cyanobacterial PSII cannot yet be excluded.

UV Kinetic Spectroscopy. At pH 6.5, the description of the O_2 signal suggests that dioxygen formation is slowed in the mutant by a factor of ~30. To verify this dramatic deceleration and to examine whether Mn reduction in the O−O bond chemistry is slowed to the same extent, we employed near-UV absorption spectroscopy at 360 nm (A_{360}) for monitoring the oxidation-state changes of the Mn complex, as described previously.[11] We note that in the O_2-forming $S_3 \rightarrow S_0$ transition of the WT PSII, the re-reduction Y_Z^{OX} is directly followed by reduction of Mn ions in the process of dioxygen formation. These three processes appear to proceed simultaneously and become visible as a decrease in the A_{360} signal (Mn reduction). The half-times of Mn reduction during the O_2-forming $S_3 \rightarrow S_0$ transition were observed to be 1.4 ms in PSII particles derived from the wild-type control strain and 43 ms in PSII particles derived from the D1-D61N mutant (Figure 8). The $t_{1/2}$ for D1-D61N is similar to the $t_{1/2}$ of PSII turnover in D1-D61N thylakoid membranes (54 ms) measured under similar conditions with the bare platinum electrode (20 °C and a low salt concentration) (Table 1.). Differences in the type of PSII preparation (thylakoid membranes vs core particles) and slightly different buffering and temperature conditions used in each experiment are the likely causes of the difference between these two values (43 ms vs 54 ms). If the transfer of an electron to Y_Z^{OX} with a half-time of 43 ms preceded an O_2 formation step with a halftime of 54 ms, then a lag phase that corresponds to the 43 ms step should be present in the electrode signal. As this is not observed, we conclude that also in D61N, O_2 release parallels the transfer of an electron to Y_Z^{OX}, Mn reduction, and O−O bond formation, consistent with earlier interpretations.[51,52]

dx.doi.org/10.1021/bi201659f | *Biochemistry* 2012, 51, 1079−1091

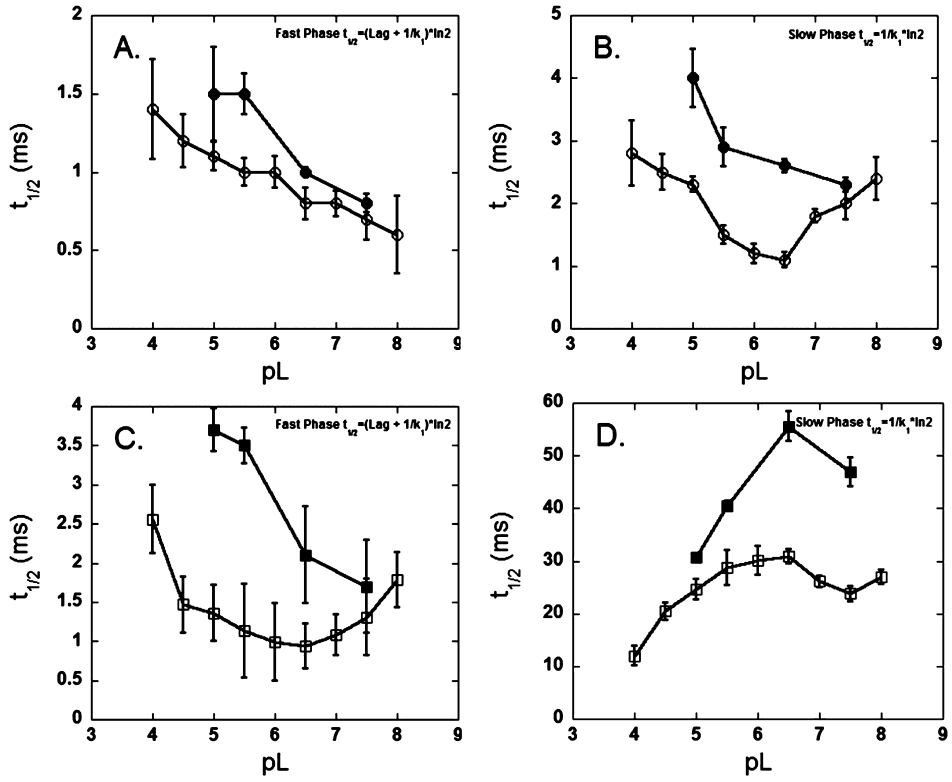

Figure 7. Time constants for the release of O_2 from thylakoid membranes. The O_2 release traces seen in Figure 4 were fit using a custom-made program (see the text and Figure 6). For this set of data, the rate of O_2 consumption was held constant. Panel A shows the time constants for the fastest of the two phases (the sum of k_1 and the extent of the lag phase) of the O_2 release curve from the wild type in H_2O (○) and D_2O (●) buffers as a function of pL. Panel B shows the time constants for the slower of the two phases (k_2). Panels C and D show the fast and slow phases of the D1-D61N time constants in H_2O buffer (□) and D_2O (■) buffers, respectively. Error bars represent the deviation from the given value required to double the sum of squares deviation between the experimental curve and the simulated curve (for more information, see the Supporting Information).

The O_2 transients detected by the bare platinum electrode exhibited a delayed rise of the signal (lag phase of ~1 ms) pointing toward formation of a reaction intermediate. In the near-UV signal, the used background removal procedure and noise contributions render the detection of a lag phase of ~1 ms before onset of the slowly rising absorption signal impossible.

The electron transfer in the D1-D61N mutant had been studied previously by near-UV spectroscopy.[24,25] In ref 24, half-times were reported for the $S_1 \rightarrow S_2$ and $S_2 \rightarrow S_3$ transitions, but not for the $S_3 \rightarrow S_0$ transition. Later the same authors reported a half-time also for the $S_3 \rightarrow S_0$ transition; its value was 13 ms and thus clearly smaller than the values of 43 ms determined herein. In ref 25, no background was subtracted, whereas we corrected for a slowly decaying background by subtraction of the transient detected on the second flash (for verification of the procedure used here, see also Figure S3 of the Supporting Information, showing period 4 oscillations). This background correction was essential for the correct determination of the half-time of the extremely slow electron transfer in the $S_3 \rightarrow S_0$ transition of the D1-D61N mutant.

Double-Flash Experiment Measuring PSII Turnover Rates. Besides the near-UV experiment, a second experiment was employed to confirm the extraordinarily slow time constants derived by the O_2 release model. The rate of PSII turnover in the $S_3 \rightarrow S_0$ transition in the D1-D61N strain was measured by a double-flash experiment using the bare platinum electrode.[32,35,53] Under a flashing light, the majority of PSII centers in a dark-adapted sample will undergo their first $S_3 \rightarrow S_0$ transition on the third flash. Four more flashes are required to reach the next $S_3 \rightarrow S_0$ transition. By gradually reducing the time interval between the third and fourth flashes, we reduce the fraction of PSII centers that have completed the $S_3 \rightarrow S_0$ transition before the fourth flash occurs. These PSII centers will be unable to complete an S-state transition during the fourth flash and will consequently not have reached the S_3 state when the seventh flash occurs. This lowers the O_2 yield of the seventh flash relative to the yield of other flashes in the series. By fitting a curve to a normalized plot of the relative amplitude of the polarographic signal on the seventh flash versus the time period between the third and fourth flashes, we can obtain an estimate of the $t_{1/2}$ of PSII turnover in the $S_3 \rightarrow S_0$ transition. With this method, a $t_{1/2}$ of 22 ms was obtained for the $S_3 \rightarrow S_0$ transition in D1-D61N thylakoid membranes using the same buffer and temperature used to measure O_2 release kinetics (Table 1). Using the O_2 release model to fit an O_2 release curve from the same sample yielded a $t_{1/2}$ of 26 ms for the longer time constant (Table 1). These values are very similar to the $t_{1/2}$ of 30.9 ms from the O_2 release curve obtained during the course of the variable-pH experiments (Figure 7). Performing the same experiment using wild-type membranes gives a time constant that is somewhat slower [3.7 ms (Table 1)] than that from the analysis of the polarographic signal. This may be true because the turnover of centers is limited by events on the acceptor side of the complex. On the basis of fluorescence measurements,[22] the D1-D61N mutant is not constrained by the acceptor side,

dx.doi.org/10.1021/bi201659f | Biochemistry 2012, 51, 1079–1091

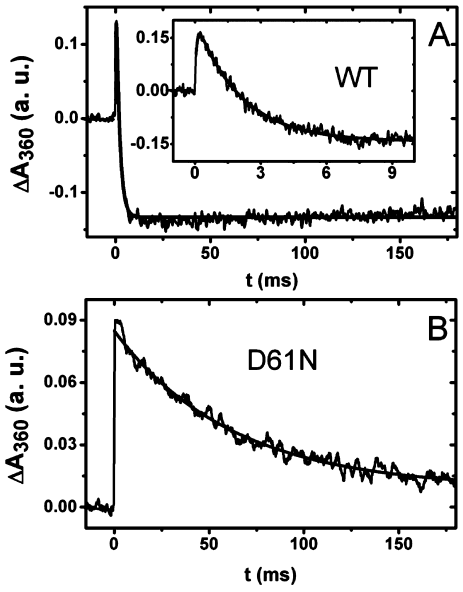

Figure 8. Absorption changes at 360 nm determined by monitoring reduction of the Mn complex in the $S_3 \rightarrow S_0 + O_2$ transition (induced by the third laser flash applied to dark-adapted PSII core particles). The difference in the absorption change transients at 360 nm induced by the third and second flashes was calculated for the WT (A) and D61N mutant (B). The difference signal does not show any slow acceptor side components, and the decay exclusively reflects the kinetics of the $S_3 \rightarrow S_0$ transition. It is fast in the case of the wild type (τ = 2.1 ms; inset of panel A), and no further kinetic component is visible in the 100 ms time range (A). The mutation generates dramatic deceleration of the decay component [τ = 62 ms (B)]. The transients induced by the first flash ($S_1 \rightarrow S_2$) and the second flash ($S_2 \rightarrow S_3$) are shown in Figure S2 of the Supporting Information.

and thus, the PSII turnover time reflects the pace of events at the WOC. Given the similarity of the estimated time constants obtained for the turnover times and the polarographic signals in the mutant, we conclude that the analysis of the O_2 signals using the physical model (eq 1) provides a reasonable approximation of the actual time constant for the $S_3 \rightarrow S_0$ transition of the WOC in the mutant. All the polarographic experiments described above were performed at the 30 °C growth temperature of the cells from which the biochemical preparations were obtained. Because measurements of the UV absorbance transients associated with Y_Z^{OX} rereduction were performed at ~20 °C, additional polarographic measurements were performed at 20 °C. Comparison of the polarographic measurements taken at 20 and 30 °C showed that the reaction has a very strong temperature dependence, but this was not explored further (Table 1).

DISCUSSION

In previous analyses, the D1-D61N mutant has been characterized as having an increased photochemical miss factor during S-state cycling and an exceptionally slow release of O_2 during the $S_3 \rightarrow S_0$ transition.[23,25] A role for the carboxyl group of D1-D61 in mediating the release of a proton from the WOC has been hypothesized,[14,19,20] and molecular modeling analysis supports this hypothesis.[16,54,55] Nevertheless, experimental tests for this important hypothesis have not been performed. Now progress has been realized via characterization of the influence of pH and the impact of deuterium isotope substitution on the kinetics of S-state cycling and O_2 release in this mutant. For analysis of O_2 release kinetics, methodological developments were required, namely, the implementation of a numerical model for simulation of O_2 transients and parameter determination by curve fitting.

The D1-D61N mutation results in a very pronounced proton/deuteron-sensitive lag phase, occurring between the actinic flash and the onset of the appearance of O_2. This lag can be directly observed using a bare platinum electrode (Figure 4C) and correlates with the fast phase in numerical fits of the O_2 signal. Importantly, the H/D isotope substitution effects on the lag and fast phase were different from the wild-type effect, indicating that the proton exit pathway is different from that in the wild type. A lag phase, occurring between the actinic flash and the onset of Y_Z^{OX} re-reduction or the appearance of O_2 during the $S_3 \rightarrow S_0$ transition, has been observed in different types of PSII samples, using several different techniques,[8,9,11,50,56] and most likely corresponds to a deprotonation of the WOC.[8,9,11] Placed in the context of these previous findings and the given fact the D1-D61N mutation results in the mechanistic recourse to an alternative proton conduction pathway, the experiments provide the first direct evidence that D1-D61 specifically facilitates proton release at this point in the reaction sequence. The results are also consistent with recent molecular dynamics simulations indicating switching of the carboxyl group of D1-D61 between different hydrogen bonding configurations relevant to the transfer process.[57]

Although D1-D61N is involved in mediating the release of protons, it does not appear to be the proposed catalytic base of the WOC because its mutational loss does not cause a severe impairment of S-state cycling efficiency (i.e., the miss factor is only moderately affected in the mutant). Previous analysis showed that the CP43-R357K mutation results in a very large miss factor in the higher S-state transitions.[15] Although the CP43-R357K miss factor (~46%) is much larger than the D1-D61N miss factor (14%), each can be attributed to a weakened ability to form and stabilize a catalytic base in the deprotonated form. The deprotonation of CP43-R357 is hypothesized to occur because of the electrostatic pK_a shift in CP43-R357 caused by the net positive charge produced by the oxidation of

Table 1. Comparison of Time Constants[a]

	$S_1 \rightarrow S_2$, UV spectroscopy (μs)	$S_2 \rightarrow S_3$, UV spectroscopy (μs)	$S_3 \rightarrow S_0$, UV spectroscopy (ms)	$S_3 \rightarrow S_0$, double-flash polarography (ms)	$S_3 \rightarrow S_0$, O_2 diffusion model (ms)	α (%), UV spectroscopy	α (%), polarography
wild type	65.8 ± 7	114.3 ± 8	1.4 ± 0.5	3.7 ± 0.2[b]	1.1 ± 0.5[b]	NA	7 ± 1[b]
D1-D61N	350.0 ± 21	447.0 ± 55	43 ± 5.1	54 ± 1 (31 ± 1[a]) (22 ± 1[b])	56 ± 1.5 (29 ± 1.3[a]) (26 ± 3.9[b])	18	14 ± 2[b]

[a]The half-times of S-state transitions were measured using UV spectroscopy at 20°C in a buffer with 5 mM NaCl. The half-time of the $S_3 \rightarrow S_0$ transition also determined using double-flash polarography and a mathematical fit of the O_2 signal with 10 mM NaCl. The polarographic measurements were also taken at 30 °C in a buffer with 10 mM NaCl (a) and at 30 °C in a buffer with 200 mM NaCl (b). NA, not available.

dx.doi.org/10.1021/bi201659f | Biochemistry 2012, 51, 1079–1091

Y_Z by $P680^+$.[58−61] The efficiency of the transfer of the proton from CP43-R357 through the PSII proton exit pathway(s) to the aqueous exterior should be critical to the stability of this deprotonated intermediate state. In D1-D61N, the proton expelled from the WOC requires an alternative, less efficient, and more time-consuming path to the aqueous exterior. A model system for proton transfer mediated by an amino acid shuttle is carbonic anhydrase. Mutants of the carbonic anhydrase proton shuttle residue, His64, which mediates the transfer of a proton from a Zn-bound H_2O to bulk solvent H_2O, exhibit a 1 order of magnitude slowing of the rate-determining proton transfer step of the CO_2 hydration mechanism that can be attributed to recourse to a less efficient alternative proton conduction pathway in place of the native pathway.[37,38] In the absence of His64, the sensitivity to external pH is diminished, not unlike the reduced pH sensitivity of the miss factor in the D1-D61N mutant. The recently determined crystal structure of PSII[12] (Figure 1) identifies four H_2O molecules potentially interacting with D1-D61, including one between D1-D61 and CP43-R357. This latter water is proposed to conduct a proton released from CP43-R357 to D1-D61N, and in the absence of a carboxyl at position 61, that proton would exit via a less efficient alternative path. Another option is that the proton exit path may start from one of the water molecules coordinated to Mn4, and D1-D61 may function as the (first) proton acceptor for the released proton. In either case, the change of this residue may therefore affect the deprotonation step and/or the subsequent proton release steps. The disruption of the normal proton conduction path via mutation would increase the time of residence of the proton in the vicinity of the WOC. This increase in the time of residence would correspondingly account for the moderate elevation of the miss factor in the D1-D61N mutant caused by an increased probability for backward reprotonation of the primary catalytic base, CP43-R357.

Interestingly, the lag phase becomes most protracted at both extremes of pH and shortest at pH 6.5 (Figure 4C). This indicates that the presumptive proton net transfer rate depends on the titration and/or structural state of protonatable groups in the exit pathway rather than being controlled by mass action exchange of protons between the site of production and the aqueous exterior. That is, if the duration of the lag were simply determined by the mass action exchange loss of a proton into the aqueous phase, then low pH, but not high pH, would be expected to prolong the lag phase. This contrasts with the behavior observed in the wild type, which did not exhibit the minimal lag phase at pH 6.5 and instead became progressively faster as the pH increased (Figure 7A). This suggests that the wild-type path is affected by mass action exchange of protons between the WOC and the aqueous exterior.

The post-lag phase O_2 release kinetics of the D1-D61N mutant is observed to be even slower than previously estimated (~13 ms[23] vs a value of >30 ms at pH 6.5 found here). Comparison with results obtained by UV−vis spectroscopy with various organisms indeed suggests that the pH dependence as well as the KIE on the slow phase may be smaller than reported herein, at least for the wild type. In the D61N mutant, however, the extended lag phase in the O_2 signal and extremely slow O_2 formation ensure that the influence of the electrode response characteristics is comparatively small. Furthermore, the overall finding of exceptionally slow O_2 release kinetics is corroborated by double-flash techniques (Table 1 and Figure S1 of the Supporting Information) and UV−vis spectroscopy (Figure 8). Still, the pH and pD dependencies are complex, and much more work will be required to understand how protons and deuterons influence the O_2 formation step. The drastic deceleration of O_2 formation may reflect the loss of a negatively charged residue near Mn_4CaO_5 as suggested previously;[24] however, current caluculations suggest that D1-D61 is protonated in the S_1 state,[54] and therefore, the electrostatic effect, if there is one, may be transient. The carboxyl moiety coordinates water molecules that are themselves ligands of Mn_4CaO_5[12] and therefore is in the proximity of redox active metals, the oxo bridges, and possible substrate molecules. It is likely important for maintaining an optimized hydrogen bonding network not only for its experimentally deduced proton relay function but also for the catalytic process of dioxygen formation occurring after the mandatory proton ejection that it facilitates.

CONCLUSIONS

Proton release throughout the S-state cycle likely functions to offset the accumulation of a positive charge on the WOC caused by the sequential removal of electrons, thereby providing a redox leveling effect on the WOC that renders the progressive oxidation steps through the higher S states thermodynamically feasible. Although D1-D61N is likely to be involved in mediating the release of protons, it does not appear to be the proposed primary catalytic base of the WOC because its mutational loss does not cause a severe impairment of S-state cycling efficiency (i.e., the miss factor is only moderately affected in the mutant). In this regard, D1-D61N is likely to provide a path for the exit of protons that have been extracted by the primary catalytic base. Placed in the context of previous findings about the probable catalytic base, CP43-R357 (one alternative being the deprotonation of a substrate water), the results are consistent with a proton ejection pathway in which proton expulsion during the initial phase of the $S_3 \rightarrow S_0$ transition serves as a hole trapping function, poising the reactants and providing the time for the comparatively slow dioxygen formation chemistry to occur with a high yield even under conditions where this chemistry is highly retarded. Proton removal during the $S_3 \rightarrow S_0$ transition thus serves a trapping function allowing the comparatively slow dioxygen formation chemistry to occur by minimizing competing recombinational losses, and D1-D61 facilitates this process. On the other hand, the strong effect of the D1-D61N mutation on the rate of O_2 release suggests that D1-D61 somehow functions in the facilitation of dioxygen chemistry, although the mechanism of its activity remains obscure.

ASSOCIATED CONTENT

Supporting Information

A more detailed explanation of the method used to fit the O_2 release transients and supplemental figures showing the results of the double-flash experiment, the near-UV absorption transients recorded from wild-type and D1-D61N PSII particles exposed to one and two flashes, and the period 4 oscillation pattern of the amplitude of the millisecond component of the near-UV absorption spectra. This material is available free of charge via the Internet at http://pubs.acs.org.

AUTHOR INFORMATION

Corresponding Author

*Address: 307 Life Sciences East, Oklahoma State University, Stillwater, OK 74078. Phone: (405) 744-7445. Fax: (405) 744-6790. E-mail: rob.burnap@okstate.edu.

Funding

This work was funded by the National Science Foundation (Grant MCB-0818371 to R.L.B.), Bundesministerium für Bildung and Forschung (BMBF, consortium 'H2 Design Cell', 03SF0355D) (to H.D.), the European Union (7th framework program, SOLAR-H2 consortium, 212508) (to H.D.), and the Edward R. & Mary M. Grula Distinguished Graduate Fellowship (to P.L.D.).

ACKNOWLEDGMENTS

We are especially indebted to Prof. Richard Debus for many useful discussions and for supplying the D1-D61N *Synechocystis* mutant.

ABBREVIATIONS

CP43, chlorophyll protein subunit of the PSII complex encoded by the *psbC* gene; D1, reaction center protein encoded by the *psbA* gene; Hepes, 4-(2-hydroxyethyl)-1-piperazineethanesulfonic acid; HBG-11, normal BG-11 growth medium buffered with Hepes-NaOH (pH 8); LED, light-emitting diode; Mn_4CaO_5, metal cluster functioning in H_2O oxidation; PSII, Photosystem II; WOC, H_2O oxidation complex of PSII; Y_Z, redox active tyrosine of the D1 protein acting as a secondary electron donor of the reaction center.

REFERENCES

(1) Kok, B., Forbush, B., and McGloin, M. (1970) Cooperation of charges in photosynthetic oxygen evolution: I. A linear four step mechanism. *Photochem. Photobiol. 11*, 457−475.

(2) Joliot, P., Barbieri, G., and Chabaud, R. (1969) Un nouveau modele des centres photochimique du systeme II. *Photochem. Photobiol. 10*, 309−329.

(3) Goussias, C., Boussac, A., and Rutherford, A. W. (2002) Photosystem II and photosynthetic oxidation of water: An overview. *Philos. Trans. R. Soc. London, Ser. B 357*, 1369−1381.

(4) Hillier, W., and Messinger, J. (2005) Mechanism of photosynthetic oxygen production. In *Photosystem II: The Light-Driven Water:Plastoquinone Oxidoreductase* (Wydrzynski, T., and Satoh, K., Eds.) pp 567−608, Springer, Dordrecht, The Netherlands.

(5) McEvoy, J. P., and Brudvig, G. W. (2006) Water-splitting chemistry of photosystem II. *Chem. Rev. 106*, 4455−4483.

(6) Sauer, K., Yano, J., and Yachandra, V. K. (2005) X-ray spectroscopy of the Mn_4Ca cluster in the water-oxidation complex of Photosystem II. *Photosynth. Res. 85*, 73−86.

(7) Dau, H., and Haumann, M. (2008) The manganese complex of photosystem II in its reaction cycle: Basic framework and possible realization at the atomic level. *Coord. Chem. Rev. 252*, 273−295.

(8) Haumann, M., Liebisch, P., Muller, C., Barra, M., Grabolle, M., and Dau, H. (2005) Photosynthetic O_2 formation tracked by time-resolved X-ray experiments. *Science 310*, 1019−1021.

(9) Rappaport, F., Lavergne, J., and Blanchard-Desce, M. (1994) Kinetics of electron transfer and electrochromic change during the redox transitions of the photosynthetic oxygen-evolving complex. *Biochim. Biophys. Acta 1184*, 178−192.

(10) Razeghifard, M. R., and Pace, R. J. (1999) EPR kinetic studies of oxygen release in thylakoids and PSII membranes: A kinetic intermediate in the S_3 to S_0 transition. *Biochemistry 38*, 1252−1257.

(11) Gerencser, L., and Dau, H. (2010) Water oxidation by photosystem II: H_2O-D_2O exchange and the influence of pH support formation of an intermediate by removal of a proton before dioxygen creation. *Biochemistry 49*, 10098−10106.

(12) Umena, Y., Kawakami, K., Shen, J. R., and Kamiya, N. (2011) Crystal structure of oxygen-evolving photosystem II at a resolution of 1.9 Å. *Nature 473*, 55−65.

(13) Babcock, G. T., Barry, B. A., Debus, R. J., Hoganson, C. W., Atamian, M., McIntosh, L., Sitole, I., and Yocum, C. F. (1989) Water oxidation in photosystem II: From radical chemistry to multielectron chemistry. *Biochemistry 28*, 9557−9565.

(14) Ferreira, K. N., Iverson, T. M., Maghlaoui, K., Barber, J., and Iwata, S. (2004) Architecture of the photosynthetic oxygen-evolving center. *Science 303*, 1831−1838.

(15) Loll, B., Kern, J., Saenger, W., Zouni, A., and Biesiadka, J. (2005) Towards complete cofactor arrangement in the 3.0 Å resolution structure of photosystem II. *Nature 438*, 1040−1044.

(16) Ishikita, H., Saenger, W., Loll, B., Biesiadka, J., and Knapp, E. W. (2006) Energetics of a possible proton exit pathway for water oxidation in photosystem II. *Biochemistry 45*, 2063−2071.

(17) Hwang, H. J., Dilbeck, P., Debus, R. J., and Burnap, R. L. (2007) Mutation of arginine 357 of the CP43 protein of photosystem II severely impairs the catalytic S-state cycle of the H_2O oxidation complex. *Biochemistry 46*, 11987−11997.

(18) McEvoy, J. P., and Brudvig, G. W. (2004) Structure-based mechanism of photosynthetic water oxidation. *Phys. Chem. Chem. Phys. 6*, 4754−4763.

(19) Murray, J. W., and Barber, J. (2007) Structural characteristics of channels and pathways in photosystem II including the identification of an oxygen channel. *J. Struct. Biol. 159*, 228−237.

(20) Ho, F. M., and Styring, S. (2008) Access channels and methanol binding site to the $CaMn_4$ cluster in Photosystem II based on solvent accessibility simulations, with implications for substrate water access. *Biochim. Biophys. Acta 1777*, 140−153.

(21) Vassiliev, S., Comte, P., Mahboob, A., and Bruce, D. (2010) Tracking the flow of water through photosystem II using molecular dynamics and streamline tracing. *Biochemistry 49*, 1873−1881.

(22) Chu, H. A., Nguyen, A. P., and Debus, R. J. (1995) Amino acid residues that influence the binding of manganese or calcium to photosystem II. 1. The lumenal interhelical domains of the D1 polypeptide. *Biochemistry 34*, 5839−5858.

(23) Clausen, J., Debus, R. J., and Junge, W. (2004) Time-resolved oxygen production by PSII: Chasing chemical intermediates. *Biochim. Biophys. Acta 1655*, 184−194.

(24) Hundelt, M., Hays, A. M., Debus, R. J., and Junge, W. (1998) Oxygenic photosystem II: The mutation D1-D61N in *Synechocystis* sp. PCC 6803 retards S-state transitions without affecting electron transfer from Y_Z to P680. *Biochemistry 37*, 14450−14456.

(25) Hundelt, M., Hays, A. M. A., Debus, R. J., and Junge, W. (1998) The mutation D1-D61N in PS II of *Synechocystis*: Retardation of ET from OEC→ Y_z^{ox} and no effect on Y_z → $P680^+$. In *Photosynthesis: Mechanisms and Effects* (Garab, G., Ed.) pp 1387−1390, Kluwer Academic Publishers, Dordrecht, The Netherlands.

(26) Debus, R. J., Campbell, K. A., Gregor, W., Li, Z. L., Burnap, R. L., and Britt, R. D. (2001) Does histidine 332 of the D1 polypeptide ligate the manganese cluster in photosystem II? An electron spin echo envelope modulation study. *Biochemistry 40*, 3690−3699.

(27) Burnap, R., Koike, H., Sotiropoulou, G., Sherman, L. A., and Inoue, Y. (1989) Oxygen evolving membranes and particles from the transformable cyanobacterium *Synechocystis* sp. PCC6803. *Photosynth. Res. 22*, 123−130.

(28) Strickler, M. A., Walker, L. M., Hillier, W., and Debus, R. J. (2005) Evidence from biosynthetically incorporated strontium and FTIR difference spectroscopy that the C-terminus of the D1 polypeptide of photosystem II does not ligate calcium. *Biochemistry 44*, 8571−8577.

(29) Tang, X. S., and Diner, B. A. (1994) Biochemical and spectroscopic characterization of a new oxygen evolving photosystem II core complex from the cyanobacterium *Synechocystis* PCC 6803. *Biochemistry 33*, 4594−4603.

(30) Burnap, R. L., Qian, M., and Pierce, C. (1996) The manganese-stabilizing protein (MSP) of photosystem II modifies the in vivo deactivation and photoactivation kinetics of the H_2O-oxidation complex in *Synechocystis* sp. PCC6803. *Biochemistry 35*, 874−882.
(31) Meunier, P. C., Burnap, R. L., and Sherman, L. A. (1995) Modelling of the S-state mechanism and Photosystem II manganese photoactivation in cyanobacteria. *Photosynth. Res. 47*, 61−76.
(32) Qian, M., Dao, L., Debus, R. J., and Burnap, R. L. (1999) Impact of mutations within the putative Ca^{2+}-binding lumenal interhelical a-b loop of the photosystem II D1 protein on the kinetics of photoactivation and H_2O-oxidation in *Synechocystis* sp. PCC6803. *Biochemistry 38*, 6070−6081.
(33) Nixon, P. J., and Diner, B. A. (1992) Aspartate 170 of the photosystem II reaction center polypeptide D1 is involved in the assembly of the oxygen evolving manganese cluster. *Biochemistry 31*, 942−948.
(34) Lavorel, J. (1976) Matrix analysis of the oxygen evolving system of photosynthesis. *J. Theor. Biol. 57*, 171−185.
(35) Bouges-Bocquet, B. (1973) Limiting steps in photosystem II and water decomposition in *Chlorella* and spinach chloroplasts. *Biochim. Biophys. Acta 292*, 772−785.
(36) Meunier, P. C. (1993) Oxygen evolution by photosystem II: The contribution of backward transitions to the anomalous behaviour of double-hits revealed by a new analysis method. *Photosynth. Res. 36*, 111−118.
(37) Tu, C. K., Silverman, D. N., Forsman, C., Jonsson, B. H., and Lindskog, S. (1989) Role of histidine 64 in the catalytic mechanism of human carbonic anhydrase II studied with a site-specific mutant. *Biochemistry 28*, 7913−7918.
(38) Jackman, J. E., Merz, K. M. Jr., and Fierke, C. A. (1996) Disruption of the active site solvent network in carbonic anhydrase II decreases the efficiency of proton transfer. *Biochemistry 35*, 16421−16428.
(39) Christen, G., and Renger, G. (1999) The role of hydrogen bonds for the multiphasic $P680^{+}$* reduction by Y_Z in photosystem II with intact oxyen evolution capacity. Analysis of kinetic H/D isotope exchange effects. *Biochemistry 38*, 2068−2077.
(40) Hyman, H. H., Kaganove, A., and Katz, J. J. (1960) The basicity of amino acids in D_2O. *J. Phys. Chem. 64*, 1653−1655.
(41) Bell, R. P. (1973) *The Proton in Chemistry*, 2nd ed., Chapman and Hall, London.
(42) Messinger, J., and Renger, G. (1994) Analyses of pH induced modifications of the period four oscillation of flash induced oxygen evolution reveal distinct structural changes of the photosystem II donor side at characteristic pH values. *Biochemistry 33*, 10896−10905.
(43) Burnap, R., Shen, J. R., Jursinic, P. A., Inoue, Y., and Sherman, L. A. (1992) Oxygen yield and thermoluminescence characteristics of a cyanobacterium lacking the manganese-stabilizing protein of photosystem II. *Biochemistry 31*, 7404−7410.
(44) Joliot, P. (1966) L'émission d'oxygène par des algues soumises à un eclairement. *J. Chim. Phys. 63*, 1423−1441.
(45) Meunier, P. C., and Popovic, R. (1991) The time for oxygen release in photosynthesis: Reconciliation of flash polarography with other measurement techniques. *Photosynth. Res. 28*, 33−39.
(46) Sinclair, J., and Arnason, T. (1974) Studies on a thermal reaction associated with photosynthetic oxygen evolution. *Biochim. Biophys. Acta 368*, 393−400.
(47) Lavorel, J. (1992) Determination of the photosynthetic oxygen release time by amperometry. *Biochim. Biophys. Acta 1101*, 33−40.
(48) Plijter, J. J., Aalbers, S. E., Barends, J. P. F., Vos, M. H., and Vangorkom, H. J. (1988) Oxygen release may limit the rate of photosynthetic electron-transport: The use of a weakly polarized oxygen cathode. *Biochim. Biophys. Acta 935*, 299−311.
(49) Christen, G., Seeliger, A., and Renger, G. (1999) $P680^{+}$* reduction kinetics and redox transition probability of the water oxidizing complex as a function of pH and H/D isotope exchange in spinach thylakoids. *Biochemistry 38*, 6082−6092.
(50) Haumann, M., Bogershausen, O., Cherepanov, D., Ahlbrink, R., and Junge, W. (1997) Photosynthetic oxygen evolution: H/D isotope effects and the coupling between electron and proton transfer during the redox reactions at the oxidizing side of Photosystem II. *Photosynth. Res. 51*, 193−208.
(51) Babcock, G. T., Blankenship, R. E., and Sauer, K. (1975) The rapid component of electron paramagnetic resonance signal II: A candidate for the physiological donor to photosystem II in spinach chloroplasts. *Biochim. Biophys. Acta 376*, 329−344.
(52) Razeghifard, M. R., Wydrzynski, T., Pace, R. J., and Burnap, R. L. (1997) $Y_z^{\bullet}$ reduction kinetics in the absence of the manganese-stabilizing protein of photosystem II. *Biochemistry 36*, 14474−14478.
(53) Diner, B. (1973) The turnover times of photosynthesis and redox properties of the pool of electron carriers between the photosystems. *Biochim. Biophys. Acta 305*, 353−363.
(54) Rivalta, I., Amin, M., Luber, S., Vassiliev, S., Pokhrel, R., Umena, Y., Kawakami, K., Shen, J. R., Kamiya, N., Bruce, D., Brudvig, G. W., Gunner, M. R., and Batista, V. S. (2011) Structural-functional role of chloride in photosystem II. *Biochemistry 50*, 6312−6315.
(55) Sproviero, E. M., Gascon, J. A., McEvoy, J. P., Brudvig, G. W., and Batista, V. S. (2008) Quantum mechanics/molecular mechanics study of the catalytic cycle of water splitting in photosystem II. *J. Am. Chem. Soc. 130*, 3428−3442.
(56) Koike, H., Hanssum, B., Inoue, Y., and Renger, G. (1987) Temperature dependence of the S-state transitions in a thermophilic cyanobacterium, *Synechococcus vulcanus* Copeland measured by absorption changes in the ultraviolet region. *Biochim. Biophys. Acta 893*, 524.
(57) Rivalta, I., Amin, M., Luber, S., Vassiliev, S., Pokhrel, R., Umena, Y., Kawakami, K., Shen, J. R., Kamiya, N., Bruce, D., Brudvig, G. W., Gunner, M. R., and Batista, V. S. (2011) Structural-Functional Role of Chloride in Photosystem II. *Biochemistry 50*, 6312−6315.
(58) Ahlbrink, R., Haumann, M., Cherepanov, D., Bogershausen, O., Mulkidjanian, A., and Junge, W. (1998) Function of tyrosine Z in water oxidation by photosystem II: Electrostatical promotor instead of hydrogen abstractor. *Biochemistry 37*, 1131−1142.
(59) Hays, A. M., Vassiliev, I. R., Golbeck, J. H., and Debus, R. J. (1998) Role of D1-His190 in proton-coupled electron transfer reactions in photosystem II: A chemical complementation study. *Biochemistry 37*, 11352−11365.
(60) Hays, A. M., Vassiliev, I. R., Golbeck, J. H., and Debus, R. J. (1999) Role of D1-His190 in the proton-coupled oxidation of tyrosine Y_Z in manganese-depleted photosystem II. *Biochemistry 38*, 11851−11865.
(61) Rappaport, F., and Lavergne, J. (1997) Charge recombination and proton transfer in manganese depleted photosystem II. *Biochemistry 36*, 15294−15302.